THE ASTROPHYSICAL JOURNAL, 441:561–567, 1995 March 10

THE INTERACTION BETWEEN HOT AND COLD GAS IN EARLY-TYPE GALAXIES

JOEL N. BREGMAN
Department of Astronomy, University of Michigan, Ann Arbor, MI 48109
AND
DAVID E. HOGG AND MORTON S. ROBERTS
National Radio Astronomy Observatory, 520 Edgemont Road, Charlottesville, VA 22903
Received 1994 June 9; accepted 1994 September 20

ABSTRACT

S0 and Sa galaxies have approximately equal masses of H I and X-ray emitting gas and are ideal sites for studying the interaction between hot and cold gas. An X-ray observation of the Sa galaxy NGC 1291 with the *ROSAT* PSPC shows a striking spatial anticorrelation between hot and cold gas where X-ray emitting material fills the large central hole in the H I disk. This supports a previous suggestion that hot gas is a bulge phenomenon and neutral hydrogen is a disk phenomenon.

The X-ray luminosity (1.5×10^{40} ergs s^{-1}) and radial surface brightness distribution ($\beta = 0.51$) is the same as for elliptical galaxies with optical luminosities and velocity dispersions like that of the bulge of NGC 1291. Modeling of the X-ray spectrum requires a component with a temperature of 0.15 keV, similar to that expected from the velocity dispersion of the stars, and with a hotter component where $kT = 1.07$ keV. This hotter component is not due to emission from stars and its origin remains unclear. PSPC observations are reported for the S0 NGC 4203, where a nuclear point source dominates the emission, preventing a study of the radial distribution of the hot gas relative to the H I.

Subject headings: galaxies: individual (NGC 1291, NGC 4203) — galaxies: ISM — galaxies: spiral — X-rays: galaxies

1. INTRODUCTION

A cold disk of atomic and molecular gas is the dominant form of interstellar material (by mass) in disk galaxies. The opposite is true in elliptical galaxies, where hot gas with temperatures $\sim 10^7$ K accounts for most of the mass (e.g., Fabbiano 1989; Sarazin 1990; Roberts et al. 1991). As in many of their other properties, Sa and S0 galaxies are intermediate systems with roughly equal amounts of hot an neutral material, with typical gas masses of 10^8–10^{10} $M_\odot$ (van Driel 1987; Canizares, Fabbiano, & Trinchieri 1987; Bregman, Hogg, & Roberts 1992). Although the hot and cold components have been studied separately in galaxies, the relationship and interaction between these two components remains a mystery. Hot gas might evaporate cold gas, or alternatively, large clouds of neutral gas might act as cooling sites for the hot material (Cowie & McKee; Macchetto & Sparks 1991). Of comparable importance may be the effect of hot gas on the star formation process in the disk. The pressure in the hot gas can be considerably greater than that in a cold disk, which may alter the star formation efficiency, the rate at which cold gas is converted into stars, or even the initial mass function (e.g., Sarazin & O'Connell 1983).

Given the possibilities for a strong interaction between hot and cold gas, one might hope to find a correlation between the global measures of each interstellar component. However, investigators have failed to find a relationship between such quantities as the X-ray and H I luminosities (or fluxes), although the large dispersion in both quantities could mask an underlying correlation (e.g., Bregman et al. 1992).

A curious feature in the H I distribution in Sa and S0 galaxies may provide a powerful clue to unraveling the interaction between hot and cold gas—the paucity of H I in the bulge region (van Driel 1987; van Driel, Rots, & van Woerden 1988; van Driel et al. 1988). This central "hole" is typically a few kpc in radius, comparable in size to the bulge component, which accounts for most of the optical light in these systems. Although CO observations of these galaxies are less extensive than the H I data, they indicate that molecular gas does not fill the central hole (compilation in Roberts et al. 1991). In some sources, such as NGC 4203, a special effort was made to observe CO in the central region, but it remains undetected (Bregman et al. 1992).

Since hot gas is associated with spherical systems such as bulges, the scarcity of cold gas in the central region suggested to us that the hot material interacts with the cold component to deplete or displace it. Were such an interaction to occur, the X-ray emission would occupy the hole in the cold gas distribution, a suggestion that can be tested by the comparison of X-ray and neutral gas images. The test of this picture was made possible when we were granted observing time on the X-ray satellite *ROSAT* (Trümper 1984) to image two nearby S0 and Sa galaxies that have holes in their H I distribution, NGC 1291 and NGC 4203. Here we describe these observations (§ 2), which are then analyzed separately and within the context of the entire interstellar content of these galaxies (§ 3).

2. THE X-RAY OBSERVATIONS

The X-ray observations were obtained with the Position Sensitive Proportional Counter (PSPC) without filters in the optical path. In the central part of the image field where our target galaxies lie, the angular resolution of the PSPC is approximately 25″. A Hubble constant of $H_0 = 50$ km s^{-1} Mpc^{-1} is used throughout.

2.1. *NGC 1291*

The brightest Sa galaxy in the Revised Shapley Ames Catalog is NGC 1291 ($B_0 = 9.17$; it is the same brightness as

another Sa galaxy, NGC 3623), which has a diameter of D_{25} = 10.5, is nearly circular (R_{25} = 0.06; an inclination less than 30° and possibly as small as 6°; van Driel, Rots, & van Woerden 1988), and a heliocentric velocity of 839 km s^{-1}. After correcting to the rest frame of the local group, the distance of NGC 1291 is 13.8 Mpc (Roberts et al. 1991), leading to M_B = −21.53. The useful exposure time was 18,298 seconds, and the background was not unusually high during any part of the exposure, so all livetime photons were used.

2.1.1. *Spatial Distribution*

The X-ray surface brightness of the galaxy decreases with radius from the center, but as fairly symmetric, to within Poisson statistics (Fig. 1). This emission extends to a radius of at least 140″, and probably beyond, but at a low signal-to-noise ratio. Within this radius, the total number of counts is 1056 ± 43 in the energy range 0.11–2.47 keV. Two images were produced in soft and hard energy bands, with the division at 0.51 keV, which makes use of the local minimum in the detector response near 0.5 keV. When comparing the 0.11–0.51 keV image to the 0.51–2.47 keV image, it is clear that the softer image extends to larger radial distances. The ratio of the soft to hard surface brightness changes by almost a factor of 4 from the center (hardest) to the outermost radii (Fig. 2). We examined whether this effect could be due to the energy dependence of the point spread function of the instrument, but find that it would be only a small effect.

To the observed surface brightness distribution we fit a model that is often used for diffuse emission from early-type galaxies, the "beta" model (e.g., Sarazin 1990), whereby the surface brightness is given by

$$I(r) = I_0[1 + (r/r_0)^2]^{-3\beta+1/2} \quad (1)$$

For proper comparison with the data, the model was convolved with an instrumental point spread function, for which we used a Gaussian of 26″ FWHM. Acceptable fits are obtained for any r_c < 1.2 kpc (<0.3), and it is impossible to obtain a meaningful best-fit value for r_c since it appears to be less than the instrumental resolution. For r_c = 0.4 kpc (6″), a best-fit model leads to $\beta = 0.51$ and $I_0 = 29.4$ counts pixel^{-1} = 1.00 × 10^{-4} counts s^{-1} arcsec^{-2} (Fig. 2); at distances beyond several core radii, the gas density is proportional to $r^{-1.53}$. This chosen X-ray core radius is consistent with the size of the optical core radius for a galaxy of this magnitude, which is 150–400 pc (Kormendy 1986).

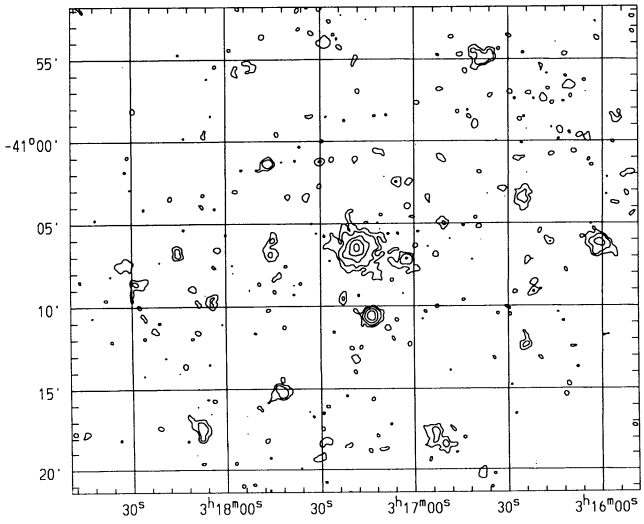

FIG. 1.—*ROSAT* PSPC X-ray image of the NGC 1291 field. Extended emission is centered on NGC 1291, but the other sources in the field are likely to be background or foreground objects. The contour levels correspond to 0.25, 0.40, 0.80, 1.6, and 3.2 counts pixel^{-1}, where each pixel is 4″ × 4″.

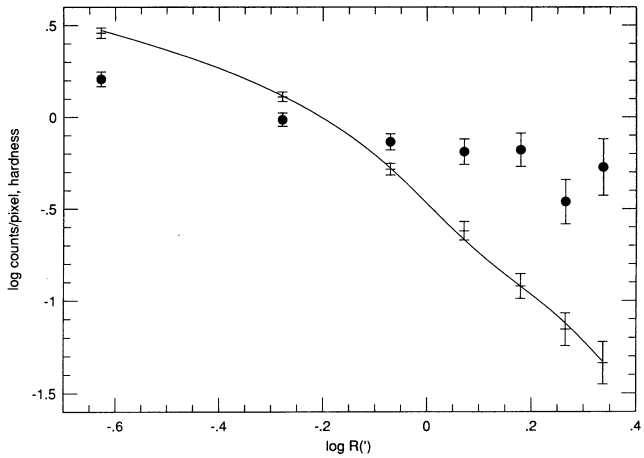

FIG. 2.—Radial X-ray surface brightness distribution for NGC 1291, along with the best fit beta model, with r_{core} = 0.1 and β = 0.51, convolved with the PSPC point response function. The hardness ratio, the log of the ratio of the 0.51–2.47 keV flux to the 0.11–0.51 keV flux (*solid circles*), decreases with radius, indicating that the emission is becoming softer at larger radius.

These derived values of β and the upper limit to r_c are similar to that found for the X-ray emission from elliptical galaxies, where $\beta \approx 0.4$–0.6 and $r_c \lesssim 2$ kpc (Forman, Jones, & Tucker 1985; Thomas et al. 1986; Canizares et al. 1987). This indicates that the spatial distribution of the X-ray emission in the bulge of an Sa is indistinguishable from that of earlier type galaxies.

2.1.2. *Spectral Analysis*

A value for the absorption column due to the Galaxy is adopted to assist with the spectral fitting. Based upon the 21 cm measurements from the Bell Labs survey, the Galactic H I column is 1.6 × 10^{20} cm^{-2}, a value that is well below the average for the Galaxy (Stark et al. 1992). There is another source in the field that is probably a background active galactic nucleus, since its spectrum is well-fit by a power law. The absorption column needed to fit a power-law spectrum to this extragalactic source is consistent with a low N_H of 1.6 × 10^{20} cm^{-2}, confirming that this is a region of a relatively low absorption column (Table 1).

Thermal Raymond-Smith models (after Raymond & Smith 1977) were fit to the signal within a diameter of 160″, assuming cosmic abundances. A one-temperature model with the above absorption column led to an unacceptable fit of the data, with χ^2 = 144 for 29 degrees of freedom; changes in the absorption column did not lead to a significant improvement in the fit. When a two-temperature model was fit to the data, the fit was improved greatly, with χ^2 = 24.2 (29 degrees of freedom) and two temperature of 0.18 keV and 1.91 keV (Fig. 3). The fit became poorer for higher absorption columns and not significantly better for lower absorption columns; we adopt the model for the following flux calculations. We note that the true representation for the plasma may include a range of temperatures, and adding more temperature components to the model will produce acceptable fits.

TABLE 1

PROPERTIES OF THREE POINT SOURCES IN NGC 4203 FIELD

Number	R.A.(2000)	Decl.(2000)	Counts	Error	α or kT	log N_{abs} (cm^{-2})	F_X[a] (10^{-13} ergs cm^{-2} s^{-1})	$F_{X,abs}$[b]	L_X (ergs s^{-1})	Comments
					The NGC 1291 Field					
1[c]	3:17:18.7	−41:06:32	1056	23	0.15 + 1.07	20.20	4.29	6.47	1.47×10^{40}	NGC 1291; diffuse emission
					0.15	20.20	2.13	3.68	8.38×10^{39}	Soft component only
					1.07	20.20	2.17	2.80	6.37×10^{39}	Hard component only
2[d]	3:17:13.9	−41:10:36	242	19	0.00	20.20	1.74	1.93	4.40×10^{39}	4.2 S of galaxy
3[c]	3:17:02.6	−41:07:10	62	14	1.00	20.20	0.19	0.24	5.54×10^{38}	3.1 W of galaxy
					The NGC 4203 Field					
1[d]	12:15:05.0	33:11:49	4827	72	1.24	20.40	21.6	40.5	4.84×10^{40}	Center of NGC 4203
2[d]	12:15:09.0	33:09:53	3091	58	1.83	20.53	12.6	41.7		2′ S of NGC 4203
3[d]	12:14:04.2	33:09:46	1039	37	1.49	20.20	3.78	7.33	2.61×10^{46}	QSO 1211+334

[a] Fluxes and luminosities are for 0.1–2.5 keV in the observer's frame.
[b] 0.1–2.5 keV flux after absorption correction.
[c] Thermal fit with Raymond-Smith plasma; T in keV.
[d] Power-law fit; α given in column six.

The total flux from the galaxy in the 0.1–2.5 keV band is 4.83×10^{-13} ergs cm^{-2} s^{-1}, the absorption corrected flux is 6.77×10^{-13} ergs cm^{-2} s^{-1}, and the luminosity is 1.54×10^{40} ergs s^{-1}. For the 0.18 keV component, the emission measure is 1.47×10^{10} cm^{-5} (this is the volume emission measure divided by $4\pi d^2$, where d is the distance to the galaxy in cm), its 0.1–2.5 keV flux is 2.4×10^{-13} ergs cm^{-2} s^{-1}, 3.7×10^{-13} erg cm^{-2} s^{-1} after absorption corrections are applied, and the luminosity is 8.5×10^{39} ergs s^{-1}. For the 1.91 keV component, the emission measure is 2.46×10^{10} cm^{-5}, the fluxes are 2.4×10^{-13} ergs cm^{-2} s^{-1}, or 2.9×10^{-13} ergs cm^{-2} s^{-1} after absorption corrections, and the luminosity is 6.7×10^{39} ergs s^{-1}. To convert these emission measures to meaningful densities, we adopt the above model for the radial distribution of the density (see § 3.2).

2.2. *NGC 4203*

The S02 galaxy NGC 4203 seemed to be a prime galaxy for our study in that it was relatively bright in X-rays (the twelfth brightest early type galaxy observed with the *Einstein Observatory*; Roberts et al. 1991) and it has a central H I hole. Its optical brightness is one-third that of NGC 1291, with a magnitude of $B_0 = 11.62$, its diameter is $D_{25} = 3.6$, and the distance derived from its recessional velocity is 22.5 Mpc (Roberts et al. 1991). The H I distribution, which extends to 250″ diameter displays an irregular hole in the center of approximately 30″–70″ diameter (van Driel et al. 1988). CO has not been detected, with an upper limit of 1.7×10^8 $M_\odot$ (Bregman et al. 1991), although NGC 4203 is a far infrared source (*IRAS*) both at 60 μm (0.6 Jy) and 100 μm (1.9 Jy; Knapp et al. 1989).

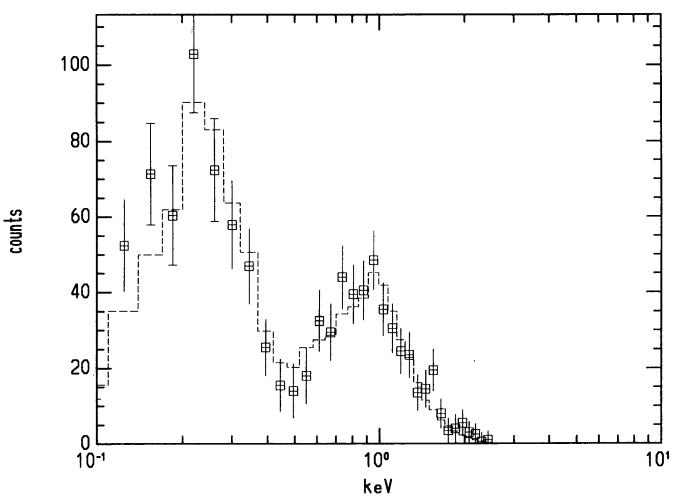

FIG. 3.—Spectral fit to the pulse-height from NGC 1291 is fit with a two temperature thermal Raymond-Smith model of cosmic abundances and with $kT = 0.15, 1.07$ keV, $\chi^2 = 19.0$.

The *Einstein Observatory* observation of NGC 4203 was brief (only 1.6 ks) so the total signal detected from a several arcminute region around the galaxy was only 135 counts. The *ROSAT* PSPC observation described here provides an improvement of a factor of 60 in the detected signal, permitting the first highly detailed X-ray study of this galaxy. With NGC 4203 in the center of the field, a *ROSAT* PSPC observation was obtained on 1991 November 24–28, and it resulted in a useful time on source of 22,959 seconds. The background was well-behaved, with no periods of high background, so the entire livetime was used.

2.2.1. *Source Detection*

The PSPC image reveals that the X-ray emission is not extended diffuse emission as was inferred from the *Einstein Observatory* observation. Instead, there are two strong point sources in the central region of NGC 4203, with the strongest source (No. 1) lying within 10″ of the optical center of the galaxy (Fig. 4). The uncertainty in the pointing (aspect solution) for the *ROSAT* PSPC is often as large as 10″, so we assume that it is truly coincident with the center of NGC 4203; we corrected for the misalignment of the PSPC by subtracting 4″ in R.A. and 10″ in Decl. from the original PSPC positions (the corrected values are given in Table 1).

The second strongest source lies approximately 2′ south of the center of NGC 4203, and is not associated with any prominent optical feature of the galaxy, although there is a blue point source within the X-ray error box and we will investigate this with future optical observations. The separation between this source and the central source is only twice the resolution of the *Einstein Observatory* IPC, so from that brief observation, the two sources were interpreted as extended emission from the early-type galaxy.

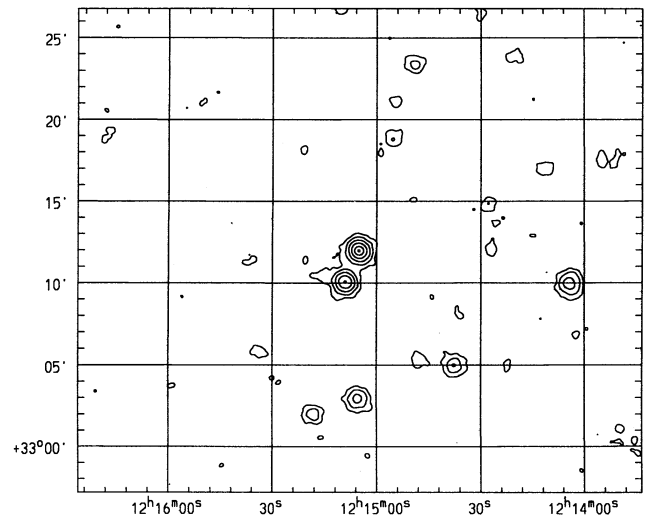

FIG. 4.—X-ray contour map of the central region of the *ROSAT* PSPC observation of NGC 4203, where the contours correspond to 0.3, 1.0, 3.0, 9.0, 25, and 44 counts per pixel and each pixel is 4″ × 4″. The brightest source in the field center is a point source in the nucleus of NGC 4203, and probably an indication of an active galactic nucleus. The other sources in the field are probably not associated with NGC 4203.

We examine whether a diffuse component of the X-ray emission is detectable in addition to the point source emission. The radial distribution of the central surce, excluding emission from the source to the south, is consistent with a point source to a radius at least 1′. It is difficult to search for diffuse emission at greater radii due to uncertainties in the background level and the shape of the point spread function (when convolved with an energy distribution). For the diffuse emission, we assume that its radial distribution is that of the "beta" model (eq. [1]) with $0.5 < \beta < 0.7$. With this diffuse emission, the radial distribution of the central point source would depart significantly from the instrumental point spread function if the diffuse emission contained 1000–2000 total counts. The more conservative upper limit of 2000 counts corresponds to an upper limit for the diffuse flux in the 0.1–2.5 keV band of 5.0×10^{-13} ergs s^{-1}, and a luminosity of less than 3.9×10^{40} ergs s^{-1} (assuming $kT = 1$ keV and cosmic abundances). This upper limit to the diffuse luminosity is still approximately four times greater than the mean value that would be predicted from the L_X-L_{opt} relationship (e.g., Bregman et al. 1992).

There are approximately 40 sources at or above the 3 σ detection threshold in the entire PSPC field, which seems to be greater than normal for a typical PSPC image where the pointing is out of the disk. However, this is a direction of lower than normal neutral hydrogen (1.3×10^{20} cm^{-2}), so the decreased absorption toward extragalactic sources is probably responsible for the abundance of sources. One source of note is the third brightest source and corresponds to the quasar 1211+334 (Hewitt & Burbidge 1987, 1989), of magnitude $B = 17.9$ and redshift $z = 1.598$ (No. 3 in Table 1). This source shows the same positional offset between the optical and the PSPC position as was found for the center of NGC 4203.

2.2.2. *Spectra and Fluxes*

The nature of the spectra of the three brightest sources are similar, and for a single-component model, are fitted best with a power-law spectra (Table 1). To apply these power-law spectra, we fit for two parameters, the absorption column and the pulse-height normalization. For sources 1 and 2, both parameters are tightly constrained, with only a narrow range of permitted values. However, for the third source, the best-fit value of the column density falls below that of the known neutral hydrogen column in that direction, approximately 1.3×10^{20} cm^{-2}. Therefore, we imposed the total absorption column (neutral plus warm ionized gas) given in Table 1. For the first two sources, the values for the absorption columns are 2–2.5 times greater than the column density of Galactic H I, so the additional absorption is probably due to warm ionized gas within our Galaxy as well as neutral and warm ionized gas within NGC 4203 and the host system of source 2.

This observation indicates that NGC 4203 is host to a modest active galactic nucleus, and recent data at other wavebands appear to support this conclusion. VLA observations reveal a weak central source at 6 cm with a flux density of 12.5 mJy (Fabbiano, Gioia, & Trinchieri 1989; Wrobel & Heeschen 1991). The emission-line gas (Bettoni & Buson 1987) was recently found to be centrally concentrated (Shields 1991) and the central line ratios are typical of the LINER class of objects (Deustua 1991).

The observed flux and spectral slope of the quasar 1211+334 (source 3) is typical of a quasar of this optical brightness. Little is known about source number 2, so we plan follow-up optical observations to help determine its nature.

3. DISCUSSION

The primary goal of this program is to understand the behavior of hot gas in the bulges of disk-bulge galaxies. Unfortunately, the strong point source in NGC 4203 prevents us from studying the hot gas in that system, so the following analysis is directed toward NGC 1291, where the hot gas provides considerable information.

3.1. *The Temperature Components*

An understanding of the origin of the two temperatures may be important to understanding the phenomena involved. In some models, the temperature of the gas is determined by the depth of the potential well, which would apply to gas that falls into the galaxy or mass loss from stars that becomes thermalized by shocks created through the random motion of the stars. If the specific gaseous thermal energy is equal to the energy is random stellar motions, then

$$T = 0.59(\sigma/300 \text{ km s}^{-1})^2 \text{ keV}$$
$$= 6.8 \times 10^6(\sigma/300 \text{ km s}^{-1})^2 \text{ K},$$

where σ is the observed one-dimensional stellar velocity dispersion. Additional heating, such as that caused by supernovae, can raise the gas temperature, although not by more than a factor of 2–3, otherwise the gas will be rendered unbound and will leave the galaxy less than 10^8 yr.

The recently measured velocity dispersion in NGC 1291 of 162 km s^{-1} (Dalle Ore et al. 1991) corresponds to a temperature of 0.17 keV, which, to within the uncertainties, is the same as the temperature of the low temperature component of 0.15 keV. Provided that that supernova heating is unimportant, the low temperature component can be the thermalized gas from stellar mass loss. There is some evidence that supernova heating may not be important. A low supernova heating rate is preferred in models that attempt to match the observed and theoretical X-ray surface brightness distribution (see review by Sarazin 1990). Also, low supernova rates are needed

to explain the weakness of the Fe emission lines in the X-ray spectrum in elliptical galaxies (Serlemitsos et al. 1993).

The higher observed temperature component, with $T = 1.07$ keV, is more difficult to explain. One possibility is that radiation from an ensemble of stars will lead to a faint but hot emission that appears diffuse at our instrumental resolution. This emission should be linearly proportional to the optical flux or luminosity of the galaxy, and so should be most apparent in the optically brightest galaxies, such as NGC 1291. Unfortunately, there is no consensus as to the stellar optical to X-ray emission ratio for a spheroidal stellar population. Forman et al. (1985) estimate the ratio to be an order of magnitude lower than that estimated by Canizares et al. (1987), and no similar estimates have yet been made from *ROSAT* data.

It is possible to discriminate between a hot gas and stellar component because if the stellar contribution of the X-ray emission is dominant, the radial surface brightness distribution of the hot component should be similar to that of the stars. The radial surface brightness distribution of the spheroid is fit by an $r^{1/4}$ law (de Vaucouleurs 1975), which in the 0.5–2.5 range, has a surface brightness proportional to $r^{-1.4}$. The radial surface brightness distribution of the hard X-ray component is proportional to $r^{-2.8}$, significantly steeper than the stellar component. This argues against the hard component being stellar in origin. Currently, we find no attractive explanation for the hard emission from NGC 1291.

3.2. *The Density Distribution and the Gaseous Mass*

We use the isothermal beta model to describe the radial distribution of the hot gas density and to calculate its mass. In this model, the parameter that describes the radial distribution of the density (β) is slightly different between the hard and soft components, with the hard component having a value of β that is greater by 0.08. Unfortunately, there are not enough photons to fit spectral models as a function of radius, thereby determining β of the two different temperature components. Consequently, we use a mean of $\beta = 0.51$, determined above (§ 2.1.1) for the entire energy band; the error introduced by this assumption is not great.

The central density is a well-determined quantity from the X-ray observations, provided that the value of the core radius is known. For the assumed core radius of 0.4 kpc (see § 2.1.1), the central gas density of the two components are

$$n_0 = 0.073 \text{ cm}^{-3} (r_c/0.4 \text{ kpc})^{-3/2}$$

for the $T = 0.15$ keV component, and

$$n_0 = 0.071 \text{ cm}^{-3} (r_c/0.4 \text{ kpc})^{-3/2}$$

for the $T = 1.07$ keV component. These values are typical of those found in other early-type galaxies, which range from 0.01–1 cm^{-3} (Sarazin 1990), and leads to instantaneous cooling times (at constant density) of 3×10^6 yr (0.15 keV component) and 7×10^7 yr (1.07 keV component). These cooling times are much shorter than a Hubble time, and for the hotter component, the cooling time is longer than the sound crossing time in the core region and at larger radii. For the cooler component, the cooling time is comparable to the sound crossing time in the central region, so this gas may not be in hydrostatic equilibrium in the central region.

The gas density has the form $n(r) = n_0[1 + (r/r_c)^2]^{-0.765}$, so that at large radius $n(r) \propto r^{-1.53}$, and the gaseous mass within radius r behaves as $M_g(r) \propto r^{1.47}$. There is no distinct outer radius to the X-ray emission, so the total gas mass is not a well-defined quantity. Within 140″, the last radius to which the X-ray emission is detected above the 3 σ level, the mass of gas is $1.7 \times 10^8 (r_c/0.4 \text{ kpc})^{1/2} M_\odot$ (0.15 keV component) and $1.7 \times 10^8 (r_c/0.4 \text{ kpc})^{1/2} M_\odot$ (1.07 keV component), or a total of $3.4 \times 10^8 (r_c/0.4 \text{ kpc})^{1/2} M_\odot$.

3.3. *Comparison to Other Early-Type Galaxies*

There are a variety of similarities between the X-ray emission from the bulge of this Sa galaxy and from earlier type galaxies, the well-studied E and E/S0 galaxies. The value of β is in the middle of the range seen in these earlier galaxies, and the central gas density is typical (Sarazin 1990), although this depends upon the assumed rather than the measured core radius. The gaseous mass is on the low end of hot gas masses determined from *Einstein Observatory* data (Roberts et al. 1991), but there are other systems with lower values of M_g.

When this galaxy is compared to the L_X-L_{opt} relationship derived from early-type galaxies, it would appear to be subluminous in X-rays by approximately a factor of 4, given its total optical luminosity (after Bregman et al. 1992). However, it may be more valid to use the luminosity of the spheroidal component of NGC 1291 when making this comparison. In this optical study of NGC 1291, de Vaucouleurs (1975) estimates that 57% of the optical light of NGC 1291 can be attributed to the spheroidal component. Using this spheroidal luminosity ($\log L_B = 10.56$) and $L_X \propto L_{opt}^a$ ($2.0 \leq a \leq 2.4$), the expected X-ray luminosity is within 25% of the observed value. Therefore, the galaxy appears to have a typical X-ray luminosity for the magnitude of the spheroidal component and the radial surface brightness distribution also is indistinguishable from E and E/S0 galaxies.

3.4. *The Relationship between the Hot and Cold Gaseous Components*

A census of the interstellar gas components in the bulge of NGC 1291 reveals that the hot material is the dominant source of gas. Neutral atomic gas is not detected in the bulge, with an upper limit to the total mass within 10 kpc (150″) of $1 \times 10^7 M_\odot$ (van Driel et al. 1988; also, reanalysis of the original data was made by us). Molecular gas has been detected in the center from the CO(1–0) line using the SEST telescope, which has a 43″ beam (Tacconi et al. 1991). However, the line width (285 km s^{-1}) of this weak CO detection (3.8 σ) is much greater than the well-measured H I line width (75 km s^{-1}; van Driel et al. 1988), a difference that is not expected and one that raises questions regarding its accuracy. The galaxy was not mapped thoroughly, but no additional CO was detected at three off-center pointings 1′, 2′, and 4′ east of the center; the estimated H_2 mass associated with the central detection is $9.1 \times 10^7 M_\odot$. The failure to detect CO easily is somewhat surprising given its 100 μm intensity of 10.7 Jy (Rice et al. 1988). Based on the correlation between CO intensity and 100 μm emission from other galaxies (Bregman et al. 1992), we would have expected a signal of approximately 200 Jy km s^{-1}, about 5 times greater than the reported measurement. These observed H I and H_2 masses are at least a few times smaller than the hot gas mass in the bulge, which is $4 \times 10^8 M_\odot$.

A final comment on this census concerns the strong far-infrared emission detection by the *IRAS* instrument (Rice et al. 1988). Emission from particularly cool dust (24 K) is consistent with the large 100 to 60 μm flux density ratio of 6.7, and for a single temperature dust model, the inferred dust mass is

approximately $5 \times 10^6\ M_\odot$. Furthermore, the dust is largely confined to the central region, with most of the emission consistent with a point source; the HWHM of the point spread function is the in-scan direction is about 45″. For a gas to dust ratio by mass 100, the gaseous mass associated with this dust would be $5 \times 10^8\ M_\odot$. The component that is closest in mass to this value is the hot gas, unless the H_2 mass has been underestimated by a factor of 6. The feasibility of the dust being associated with the hot gas is considered below.

The anticorrelation between the hot and neutral atomic gas is one of the most striking results of this work. The total atomic H I mass within the galaxy is considerable, $3.2 \times 10^9\ M_\odot$, but nearly all of that lies within the disk rather than in the bulge region (Fig. 5 [Pl. 11]). Moving radially inward from the disk, the H I column density drops precipitously in the 12–20 kpc (3′–5′) range and is undetectable within 10 kpc (2.5) of the center (Fig. 6), which is where the light from the bulge component begins to dominate and where the X-ray emission becomes detectable. *The X-ray emitting material appears to fill the central hole in the* H I *gas.* This striking anticorrelation must be tempered by the possibility that the total neutral gas surface brightness is poorly known because the 3 σ upper limit to the H_2 surface mass density is approximately 11 $M_\odot$ pc^{-2}, much greater than the measured surface mass densities in hot gas or H I (0.1–1 $M_\odot$ pc^{-2}). Consequently, it is possible that the molecular surface mass density rises as the H I decreases so that there is no hole in the neutral gas content to be filled in by the hot gas. If this occurs, the high pressure of the hot gas might assist in converting H I to H_2. At 10 kpc, where the H I has become undetectable, the hot gas pressure is already $P/k \sim 10^4$ K cm^{-3} and P/k rises by two orders of magnitude toward the center, which are pressures comparable to those in molecular clouds.

The absorption column density determined from the X-ray observations places useful limits on the surface mass density of neutral gas in the bulge of NGC 1291. Neutral gas with a projected covering factor near unity will absorb X-ray emission from the far side of the NGC 1291. The absorption column deduced from the X-ray observations is 1.6×10^{20} cm^{-2} (§ 2.1.2), which is consistent with the Galactic H I column in the direction. Therefore, any absorption within NGC 1291 must have a column density of less than 0.6×10^{20} cm^{-2}, or $<0.5\ M_\odot$ pc^{-2}. The H I observations in the bulge of NGC 1291 are well below these limits, although the CO detection would imply a column density of 1.8×10^{21} cm^{-2} if spread smoothly across the SEST beam. The CO observations can be made consistent with the upper limits on internal absorption if the molecular clouds have a small area filling factor, occupying only a fraction of the beam area.

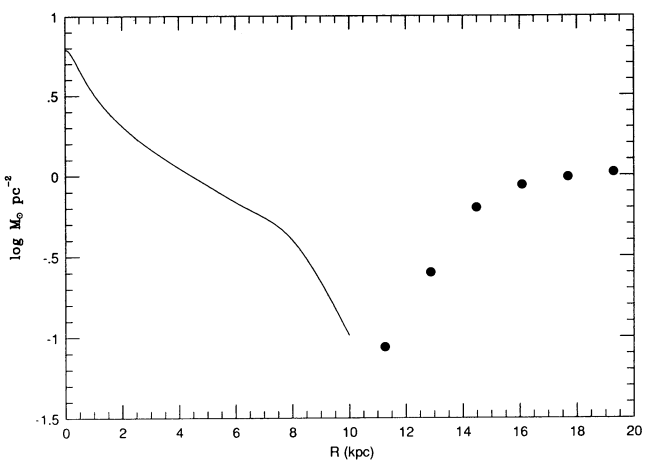

FIG. 6.—Radial surface mass density plots of H I (*filled circles*) and X-ray gas (*solid line*) as a function of radius in NGC 1291. The uncertainties at the lowest flux levels for H I are dominated by systematic effects in the instrument and data reduction, but no flux is detected within 10 kpc. The X-ray emission appears to fill the central hole in the H I distribution.

An original motivation for making these observations was to search for the signature of a thermal interaction between the X-ray emitting gas and the H I. Interactions between hot and cold phases can be divided into two broad cases, one where the two phases are thermally isolated and the other in which they exchange energy, possibly through conduction of turbulent mixing. Fortunately, these two cases lead to different signatures for the X-ray spectrum at the locations where neutral and hot gas overlap. When conduction or turbulent mixing is effective, one phase can be converted to the other, leading to an anticorrelation between phases. In this thermally coupled case, there is a local cooling of the hot material where it meets neutral gas (e.g., H I), leading to a softening of the X-ray spectrum relative to hot gas regions without neutral gas. The opposite effect, a hardening of the X-ray spectrum, occurs when the two phases are thermally isolated, because the primary consequence of the cold component is to absorb X-rays emitted by hot gas on the far side of the galaxy, provided that the covering factor of the neutral gas is greater than 10%–20%. Significant softening of the X-ray spectrum is observed with increasing radius (§ 2.1.1; Fig. 2), as the H I ring is approached, and this might be interpreted as thermal coupling between the two phases. As the hot gas has a greater column density than the H I in this bulge region, thermal mixing might deplete the H I content of the disk, leading to the paucity of H I observed in the bulge. Whereas this may be the correct explanation of events, there are several problems. First, H I is undetected in the region where the X-ray spectral softening occurs, so we cannot be confident that there is any gas to interact with the hot medium. Second, we do not understand the origin of the hotter X-ray emitting component, and until it is understood, it may be premature to attribute a change in the relative strength of this component to thermal mixing.

Finally, we speculate as to the importance of the emission from the dust. It is possible that the dust is associated with CO (detected and undetected), although star formation is nearly absent in the bulge (Caldwell et al. 1991; J. Gallagher 1994, private communication), which usually accompanies significant far-infrared emission. An alternative possibility is that the dust is associated with the hot gas rather than the cold gas. This would occur as gas and dust shed by stars undergoes shock heating with other gas (either the hot bulge gas or mass lost from another star), a process that effectively heats the gas but does not destroy the dust (at these gas densities). One of the attractions of this explanation is that the gas-to-dust ratio is about 70 (using all the hot gas in the bulge), which is characteristic of the Galactic value. Sputtering of the dust by the gas will heat and destroy the dust, and only large ($>0.5\ \mu$m) grains will survive for longer than the radiative cooling time of the gas (after Ostriker & Silk 1973; Dwek & Arendt 1992). Heating of the dust by the hot thermal electrons would produce a far infrared luminosity $\sim 10^{40}$ ergs s^{-1}, far less than the far infrared luminosity from the bulge, which we estimate to be in the range $2–4 \times 10^{42}$ ergs s^{-1}, based on the *IRAS* data from Rice

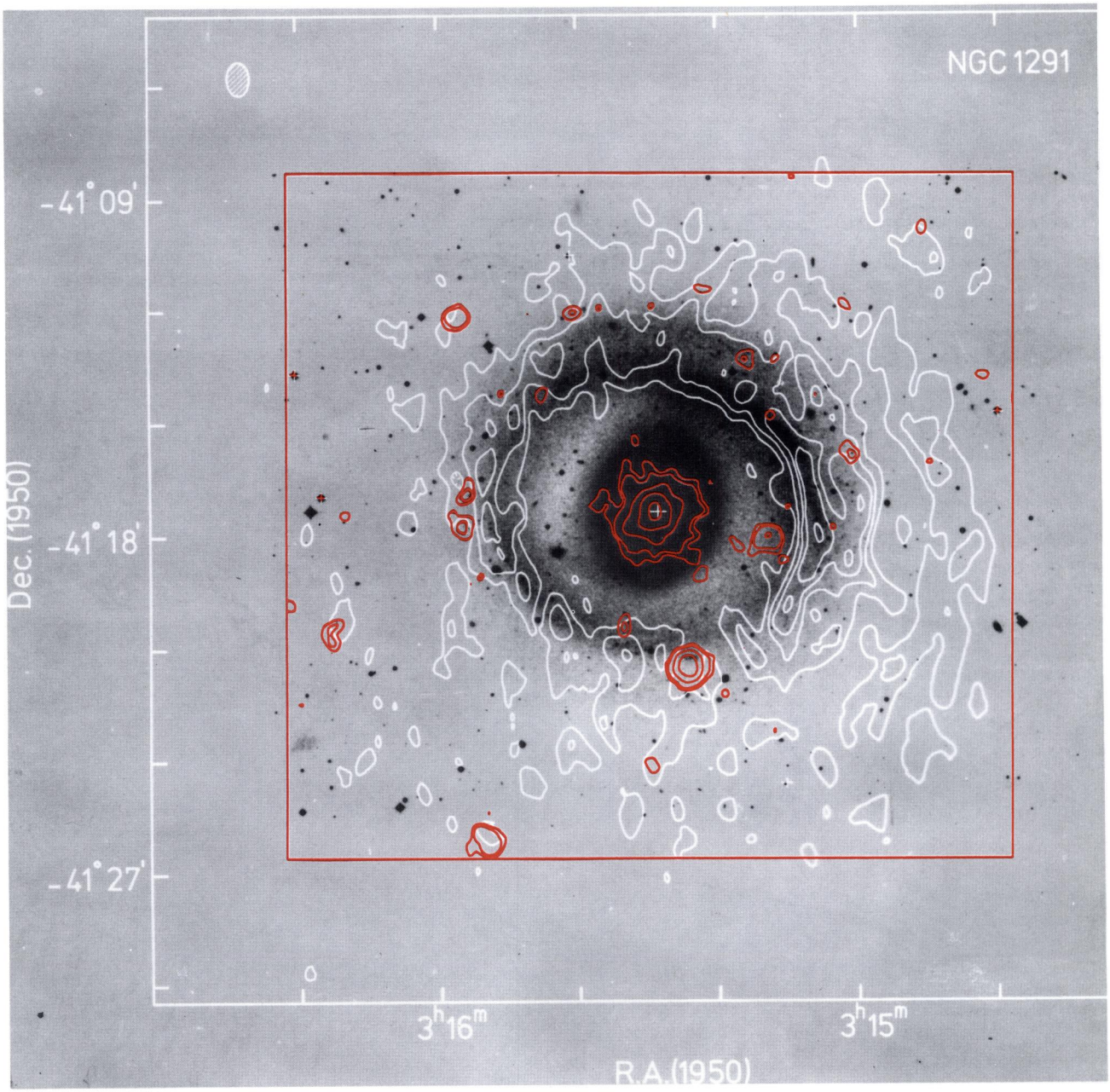

FIG. 5.—Blue optical image of NGC 1291 with the H I and X-ray emission contours superposed. The H I map has a resolution of 48″ × 48″ and the contour levels, in white, are at $N_{HI} = 0.66, 1.3, 2.0, 2.6, 3.3 \times 10^{20}$ cm^{-2} (van Driel et al. 1988); the beam size is shown in the upper left. The X-ray emission in the 0.11–2.47 keV energy band has a resolution of about 25″, and the contour levels, in red, are those given in Fig. 1. The X-ray emission is coincident with the bulge, a region with no detectable H I emission.

et al. (1988). The emission is most likely powered by absorption of starlight from the bulge, as it would require the absorption of less than 1% of the bolometric optical luminosity of the bulge.

4. CONCLUSIONS

We have observed the X-ray emission from two Sa/S0 galaxies in order to study the nature of the emission, whether it displaces the H I, creating a central H I hole, and whether the hot and cold gases interact through mixing or thermal conduction. Two galaxies were observed, NGC 4203 and NGC 1291, but the X-ray emission from NGC 4203 is dominated by a strong central point source, so the extended emission could be studied only in the NGC 1291. The spatially resolved X-ray emission from NGC 1291 comes entirely from the bulge region, where this smoothly varying emission has a radial surface brightness distribution ($\beta = 0.51$) that is typical of the X-ray emission in elliptical galaxies. Also, the X-ray luminosity is typical of elliptical galaxies of the same optical luminosity, provided that we consider the optical luminosity of the bulge only.

A spectral analysis of the PSPC data for NGC 1291 suggests the presence of a two temperature medium with a hot ($kT = 1.07$ keV) and a cooler ($kT = 0.15$ keV) component. The temperature of the cooler component is the same as that expected when gas is shed by stars and thermalized in the bulge (0.17 keV, assuming isotropic orbits for the stars). However, the temperature of the hotter component is above the escape temperature from the bulge, yet it has a spatial distribution similar to the cooler X-ray component. It is unlikely that this emission is from an ensemble of stars because the predicted stellar X-ray flux is below the observed value and the radial surface brightness distribution of the starlight is much shallower than that of the X-ray component. The origin of this hard X-ray component remains unclear.

Neutral hydrogen is plentiful in the disk of NGC 1291, but there is a large central hole where H I remains undetected ($R < 10$ kpc). This hole is large compared to that of normal spirals, and van Driel et al. (1988) notes an unusually rapid decrease in the H I intensity at the edge of the hole (near $R = 13$ kpc). The region in which H I is absent corresponds to the presence of the X-ray emitting gas, suggesting a strong anticorrelation between the two components. These data support the view that the presence of hot gas is a bulge phenomenon and the presence of cold gas is a disk phenomenon (Bregman et al. 1992). This anticorrelation may occur because the hot and neutral phases prefer not to be cospatial, with thermal mixing or conduction leading to the dominance of one component. Alternatively, the high pressures in the bulge due to the hot gas ($P/k \sim 10^6$–10^4 K cm^{-3} from the center to the edge of the bulge region) may have led to H I being converted to H_2. A weak CO detection has been reported for the central region (Tacconi et al. 1991; upper limits are reported away from the nucleus). Because CO measurements are relatively less sensitive at measuring a mass surface density of H_2 than 21 cm measurement at determining a mass surface desity of H I, H I in the bulge could have been converted to H_2 and would escape detection.

A strong 60 and 100 μm signal is seen from the bulge, and since the emission is unresolved at 60 μm, it must be confined to the central 2 kpc in radius. The gas-to-dust ratio is normal if we use the hot gas, and we suggest that the dust was shed by the stars, along with the gas that became the hot X-ray emitting medium. The hot gas has a minor heating effect on the dust, with most of the dust heating due to absorption of starlight from bulge stars (the total far-infrared luminosity, $\sim 3 \times 10^{42}$ ergs s^{-1}, is less than 1% of the bolometric optical luminosity of the bulge).

In the future, we hope to report upon additional X-ray observations of other Sa galaxies to examine whether a H I hole generally corresponds to the region of hot gas emission, and whether the hot gas has multiple temperature components.

We would like to thank Wim van Driel and Arnold Rots for their assistance in obtaining and reanalyzing the H I data. In addition, we thank Jay Lockman, Craig Sarazin, Jay Gallagher, Nelson Caldwell, Hugo van Woerden, Renzo Sancisi, Pat Smiley, and George Kessler for their scientific advice and technical assistance. J. N. B. would like to acknowledge support from NASA under contracts NAGW-2135 and NAG 5-1955. The NRAO is operated by Associated Universities, Inc., under cooperative agreement with the NSF.

REFERENCES

Bettoni, D., & Buson, L. M. 1987, A&AS, 67, 341
Bregman, J. N., Hogg, D. E., & Roberts, M. S. 1992, ApJ, 387, 484
Caldwell, N., Kennicutt, R., Phillips, A. C., & Schommer, R. A. ApJ, 370, 526
Canizares, C. R. Fabbiano, G., & Trinchieri, G. 1987, ApJ, 312, 503
Cowie, L. L., & McKee, C. F. 1977, ApJ, 211, 135
Dalle Ore, C., Faber, S. M., Jesus, J., Burstein, D., & Stoughton, R. 1991, ApJ, 366, 38
Deutsua, S. 1991, Ph.D. thesis, Univ. Michigan
de Vaucouleurs, G. 1975, ApJS, 29, 193
Dwek, E., & Arendt, R. G. 1992, ARA&A, 30, 11
Fabbiano, G. 1989, ARA&A, 27, 87
Fabbiano, G., Gioia, I. M., & Trinchieri, G. 1989, ApJ, 347, 127
Forman, W., Jones, C., & Tucker, W. 1985, ApJ, 293, 102
Hewitt, A., & Burbidge, G. 1987, ApJS, 63, 1
———. 1989, ApJS, 69, 1
Kormendy, J. 1986, in Nearly Normal Galaxies, ed. S. M. Faber (Heidelberg: Springer), 163
Knapp, G. R., Guhathakurta, P., Kim, D.-W., & Jura, M. 1989, ApJS, 70, 329
Macchetto, F., & Sparks, W. B. 1992, in Morphological and Physical Classifications of Galaxies, ed. G. Longo, M. Capaccioli, & G. Busarello (Dordrecht: Kluwer), 191
Ostriker, J. P., & Silk, J. 1973, ApJ, 184, L113
Raymond, J. C., & Smith, B. W. 1977, ApJS, 35, 419
Rice, W., et al. 1988, ApJS, 68, 91
Roberts, M. S., Hogg, D. E., Bregman, J. N., Forman, W. R., & Jones, C. 1991, ApJS, 75, 751
Sarazin, C. L. 1990, in The Interstellar Medium of External Galaxies, ed. H. A. Thronson, Jr. & J. M. Shull (Dordrecht: Kluwer), 201
Sarazin, C. L., & O'Connell, R. W. 1983, ApJ, 268, 552
Serlemitsos, P. J., Loewenstein, M., Mushotzky, R. F., Marshall, F. E., & Petre, R. 1993, ApJ, 413, 518
Shields, J. C. 1991, AJ, 102, 1314
Stark, A. A., Gammie, C. F., Wilson, R. W., Bally, J., Linke, R. A., Heiles, C., & Hurwitz, M. 1992, ApJS, 79, 77
Tacconi, L. J., Tacconi-Garman, L. E., Thornley, M., & van Woerden, H. 1991, A&A, 252, 541
Thomas, P. A., Fabian, A. C., Arnaud, K. A., Forman, W., & Jones, C. 1986, MNRAS, 222, 655
Trümper, J. 1984, Phys. Scripta, T7, 209
van Driel, W. 1987, Ph.D. thesis, Rijk, Univ. Groningen
van Driel, W., Rots, A. H., & van Woerden, H. 1988, A&A, 204, 39
van Driel, W., van Woerden, H., Gallagher, J. S., & Schwarz, U. J. 1988, A&A, 191, 201
Wrobel, J. M., & Heeschen, D. S. 1991, AJ, 101, 148